SMALL ANGLE X-RAY DIFFRACTION STUDIES OF MUCOPOLYSACCHARIDES IN COLLAGEN

R. LAM, W. J. CLAFFEY, AND P. H. GEIL, *Department of Macromolecular Science, Case Western Reserve University, Cleveland, Ohio 44106 U.S.A.*

ABSTRACT Small angle X-ray diffraction (SAXD) was used to locate mucopolysaccharides (MPS) at regular intervals along the collagen axis under physiological conditions. Ruthenium red was used to stain the MPS specifically. The difference in electron density between ruthenium red-stained and unstained moist native rat tail tendon should correspond to the position of the MPS. This difference was calculated from the SAXD intensity data by using difference Fourier transform calculations. Phases calculated independently from the amino acid sequence of collagen by two laboratories were used in this calculation, and the results were compared. At least four to seven bands of MPS per 660 Å were found at regular intervals along the collagen axis. Some of these bands match in position to the cross-striations observed by freeze-etching. Electron micrographs of ruthenium red-stained native fibrils also showed bands close in position to the ones calculated.

INTRODUCTION

Electron microscopy has suggested the possibility that mucopolysaccharides (MPS) are located at periodic intervals along the collagen fibril axis. By thin sectioning and alcian blue staining, Ruggeri et al. (1) found bands of proteoglycans at 640 Å intervals at right angles to the collagen axis. Using ruthenium red, several groups of investigators (2–5) found similar bands of proteoglycans attached orthogonally to the collagen fibril. Nakao and Bashey (3) reported the $d - e_2 - a_4$ region is electron dense. Serafini-Fracassini and Smith (6) observed belts of beaded structures stained by bismuth nitrate corresponding to the positions of the a and b_1 bands of phosphotungstic acid (PTA)-stained collagen. Yoshihara[1] also found noncollagenous fibrous materials attached regularly to collagen by shadowing and staining. Since the materials may clump together during preparation and shrink under the electron beam, we suggest that freeze-etching[2] and small angle X-ray diffraction (SAXD) might be better techniques to locate the MPS under native conditions. In particular, if there is matter periodically located at large intervals, SAXD would be the most suitable method for studying them under physiological conditions. Likewise, freeze-etching, although also subject to possible artifact formation, is at least subject to a different type of artifact than the fixing, staining, and drying, etc., used for prior electron microscope studies and should be more suitable for correlation with SAXD results.

[1]Yoshihara, T. Unpublished observation.
[2]Lam, R. K., and P. H. Geil. 1977. Manuscript in preparation.

In the past attempts (7–11) have been made to analyze the electron density distribution along the collagen fibril axis using SAXD. Kaesburg and Shurman (7) and later Ericson and Tomlin (9) tried using Patterson distribution functions on native, PTA-, and iodine-stained materials. Kaesburg and Shurman (7) suggested that the wet, unstained collagen has a dense band with a width of 53% of the total period, whereas the PTA-stained collagen has eight bands per period in electron microscope and X-ray studies. They could not specify the location of these bands within the period. Ericson and Tomlin (9) also interpreted the small angle X-ray data as showing the presence of a band with higher density and an interband with lower density per period. The width of the latter band was determined as 0.46 of the 660 Å period. X-ray patterns from stained tendons yielded similar Fourier transforms for all of the stains (iodine, PTA, osmium tetroxide, and silver): a pair of dense bands 0.4 D apart (D being the collagen 660 Å period), one at each end of the overlap.

A major problem in any direct interpretation of the SAXD pattern is the determination of the phases of the various reflections. Tomlin and Worthington (8) assumed that collagen has a centrosymmetric center, i.e., the gap/overlap is 0.5/0.5 and thus simplified the determination of the phases involved. Using these values and the measured intensities, they inferred that the repeating unit was a step density function with an overlap-to-gap ratio of 0.47/0.53 or 0.53/0.47. Later, Chandross and Bear (11) attempted to derive phases from electron densities obtained from electron micrographs of PTA-stained fibers. The validity of this as applied to wet, native collagen is questionable. First, the period is known to contract from 660 Å in the native state to 640 Å in the dried state. Their method would not be valid unless there is uniform shrinkage throughout the period on drying. This is not always the case, since some regions are known to be more disordered than others and nonuniform shrinkage may easily result. Secondly, and of more concern, the electron micrographs they used were those of PTA-stained materials. PTA staining would change the electron densities at the stainable regions drastically and thus change the overall electron density distribution along the period. Thus, one would not expect to obtain the correct phases necessary for structural determination.

With the completion of the determination of the amino acid sequence (12, 13), appropriate phases have been calculated directly by Claffey in our laboratory (14) and by another group of workers (15). Claffey (14) calculated the axial projection onto the molecular axis of electron densities using the Hodge-Petruska-Smith microfibril model. Based on matching amino acid sequences with staining patterns of segment long spacing (SLS), native, and reconstituted collagen (16–19), it has been proposed that the staggering of the Hodge-Petruska model should be in the vicinity of 234 amino acids. Since this stagger is not accurately known, Claffey (14) calculated the projection for different staggers of the sequence and found that the structure factors calculated had a minimum residual R value of 0.28 at a stagger of 236 or 237 amino acids. He could not distinguish between these two staggers. Some differences were observed between the electron densities obtained from the two staggers and the electron density obtained using observed intensities and calculated phases. These differences were mainly

at the telopeptide regions. This is expected since it was assumed in the calculations that the telopeptide regions were helical, whereas in the actual case, these are nonhelical and have been suggested to be contracted with respect to the helix repeat. These results suggest that the phases so obtained are reasonable and should be able to serve as a satisfactory basis for the interpretation of SAXD of unstained collagenous materials. We also note that the unstained collagen used for the diffraction patterns contains MPS; thus one would not expect complete agreement between calculated and observed intensities.

Hulmes et al. (15) also used the Hodge-Petruska-Smith microfibril model to calculate phases such that the SAXD patterns could be analyzed. Although Claffey (14) used only the amino acid sequence of the α1 chain, Hulmes et al. included portions of the α2 sequence that had been completed and made a pseudo-α2 chain such that each tropocollagen molecule in their model had two α1 chains and one pseudo-α2 chain.

Since the conformations of the telopeptide regions were not known, they put in a variable parameter that could extend and contract the telopeptide regions in their model. They found that the calculated intensities for the extended conformation of the telopeptides did not agree very well with observed intensities; therefore, this model was ruled out. Difference Fourier synthesis between observed and calculated intensities was used as a criterion for the best model, i.e., the one that gave a difference Fourier synthesis as close to zero as possible. They concluded the best model was one with a stagger of 234 amino acids and with the telopeptides somewhat contracted. The disaccharides known to exist (20, 21) in each α1 chain of collagen were not included in their electron density model, and thus were assumed not to affect the phases.

Since the two sets of phases were somewhat different and it was not possible to choose arbitrarily between the two, they were both used in our difference Fourier transform calculations to give two sets of results. These results were then correlated to electron microscope studies of ruthenium red-stained native collagen fibrils.

The availability of these new phases made it possible to determine more accurately the electron density distribution along the collagen fibril axis. However, of more immediate interest is the possibility of using difference Fourier transform calculations to determine the location of MPS if they can be preferentially stained. Here one compared the patterns of stained and unstained collagen using Eq. 1, and thus located any MPS periodically present along the collagen axis.

$$\Delta\rho(x) = \Sigma(F_s - F_u) \cos (2\pi hx - \phi(h)) \qquad (1)$$

where $\Delta\rho(x)$ = electron density difference between stained and unstained samples; F_s = structure amplitude of stained samples; F_u = structure amplitude of unstained samples; ϕ = phases; h = diffraction order; x = fraction of period.

In using the phases obtained from the amino acid sequence, two assumptions were made. First, it was assumed that the MPS (if any), disaccharides, and possibly glycoproteins made minor contributions to the scattering and did not affect the phases significantly. Secondly, the staining of the MPS by ruthenium red was also assumed

not to affect the phases. This was the central assumption made in doing the difference Fourier calculations. For both assumptions to be valid, the amount of MPS present had to be relatively small compared to the amount of collagen that is diffracting. However, if it were too small, we might not be able to detect it. A tissue that met this requirement is rat tail tendon (RTT), which contains <0.1% MPS. Since RTT gives a well-oriented small angle X-ray pattern, it was used in our research.

The greatest problem in applying this technique for location of MPS was the reliability of MPS-specific stains available to date. Bouteille and Pease (22) had suggested the use of PTA at pH < 2 for specific staining. However, previous work in this laboratory had demonstrated that under such conditions, the collagen itself was also stained. Both alcian blue and bismuth nitrate had been advocated as MPS-specific stains in thin sectioning (1, 6). But under the harsh acidic conditions (pH < 2) required for working with these stains, the collagen fibrils were partially destroyed, affecting intensity measurements. The problem was that any staining method used probably depends on ionic interaction of a positively charged stain with negatively charged MPS; and the presence of other anions (e.g. proteins) could also interact with the stain. To date, the most suitable stain at physiological pH seemed to be ruthenium red (23, 24) and it was this we had used.

EXPERIMENTAL

CuKα radiation from a Picker microfocus X-ray generator (Picker Corp., Cleveland, Ohio) was used with a Franks double-mirror camera. To obtain the first order diffraction of collagen, the film was placed 33 cm from the second mirror. 48-h exposure times were used. A pack of three films (Ilford Industrial G, Ilford Ltd., Ilford, Essex, England) was used for each run. For higher order reflections, the film-to-specimen distance was shortened to 15 cm and 8 cm for still higher orders.

Native RTT were rinsed and stored in Ringer's solution at 4°C. One tendon was clamped under slight tension in a sample holder that permitted the bottom end of the bundle of fibers to be in contact with Ringer's solution and kept at high humidity by ¼-mil Mylar windows (Chemplex Industries, Inc., East Chester, N.Y.).

Some tendons were stained with 1,000 ppm ruthenium red (Polysciences, Inc., Warrington, Pa.) in 0.02 M Na cacodylate buffer at pH 7.3 for 24 h at 4°C.

Intensity measurements were taken with an E.D.P. microdensitometer (Photometrics, Inc., Lexington, Mass.). To compare intensities obtained from different sets of films, the intensities of the third-order reflection for both stained and unstained samples were used as standard and the intensities of all other orders of the set were ratioed against it.

It is assumed that the integral intensity is proportional to the peak heights; therefore, in all cases, peak heights were measured.[3] The two sets of intensities from the stained and unstained experiments were then adjusted such that the first order of the untreated set was given an arbitrary value of 1,000, and the treated set was then adjusted such that the total intensities for 25 reflections of both sets were equal.

For electron microscopy, the RTT were mechanically dispersed with a Waring blender (Waring Products Div., Dynamics Corp. of America, New Hartford, Conn.) and stained with 1,000 ppm ruthenium red in Na cacodylate buffer for several hours. Excess stain was removed by drawing off with filter paper and the grids were rinsed several times with buffer and allowed to dry

[3]The line widths of the reflections of stained and unstained samples were the same to <10%.

before being studied under the electron microscope. Some fibrils were freeze-dried, smoked with MgO, and then shadowed with platinum.

To obtain thin sections, ruthenium red-stained intact tendons were dehydrated stepwise in increasing concentrations of hexylene glycol in 0.2 M Na cacodylate buffer. They were then embedded in Spurr's low-viscosity epoxy and sectioned with a Reichert microtome (C. Reichert Optical Works, Vienna, Austria).

Reconstituted RTT was prepared by first dissolving RTT in dilute acetic acid overnight at 4°C. The collagen solution was then filtered with glass wool. Ammonium hydroxide was added to the solution to precipitate the collagen. After precipitation, the suspension was centrifuged at 7,200 rpm for 30 min and the supernate was discarded. The residue was washed with distilled water twice and then dispersed with a Waring blender. This procedure was repeated twice. A drop of reconstituted RTT was placed on a copper grid, allowed to dry, and then stained with ruthenium red for electron microscope observations. All electron microscope work was done with a JEM 100B electron microscope (JEOL Ltd., Tokyo, Japan).

RESULTS AND DISCUSSIONS

The intensities of 25 diffraction orders from SAXD patterns for ruthenium red-stained and unstained moist RTT are given in Table I. These intensities have been normalized so that the total intensities of the stained and unstained data are in a ratio of 1:1. The

TABLE I
RELATIVE INTENSITIES OF RUTHENIUM RED-STAINED AND UNSTAINED MOIST NATIVE RTT

Order h	Unstained RTT	Ruthenium red-stained RTT
1	1,000.0	926.0
2	6.0	6.0
3	114.0	140.0
4	6.0	4.0
5	29.0	50.0
6	6.0	7.0
7	5.0	12.0
8	3.0	7.0
9	11.0	17.0
10	2.0	4.0
11	1.0	3.0
12	3.0	5.0
13	0.0	0.0
14	0.0	0.0
15	2.0	2.0
16	0.5	0.5
17	0.5	0.5
18	0.5	0.5
19	0.0	0.0
20	3.0	3.0
21	3.0	2.0
22	2.0	1.0
23	0.0	0.0
24	0.0	0.0
25	0.5	0.5

relative intensities of the unstained data are in agreement with those reported by Tomlin and Worthington (8) for moist RTT. No SAXD intensity data is available for comparison with that from the ruthenium red-stained samples.

The two sets of phases calculated by Claffey (14) and Hulmes et al. (15) are listed in Table II. Both sets of phases were used in the difference Fourier transform calculations, carried out with Eq. 1.

The electron density difference ($\Delta\rho(x)$) should correspond to ruthenium red-stained entities located periodically along the collagen fibril. A plot of this density difference obtained by using the phases by Claffey (14) is shown in Fig. 1. Based on Claffey's phases (14), we obtained the electron-dense peaks at 0.00, 0.11, 0.20, 0.34, 0.44, 0.60, 0.70–0.74, and 0.84 fractions of the period. Fig. 2 shows the density difference calculated using phases by Hulmes et al. (15). Based on these phases, the electron-dense peaks are at 0.00, 0.16, 0.18, 0.28, 0.41, 0.53, 0.60–0.64, 0.70, and 0.83 fractions of the period.

There is agreement on the major peaks at 0.0, 0.4, and 0.8 fractions of the period between the two calculations. These three peaks would correspond to the positions of

TABLE II

PHASES CALCULATED FROM THE AMINO ACID SEQUENCE OF COLLAGEN BY CLAFFEY (14) AND HULMES ET AL. (15)

Order h	$\phi(h)$ in radians (14)	*$\phi(h)$ in radians (15)
1	1.485	1.676
2	−0.172	2.498
3	0.959	1.259
4	1.159	−2.407
5	0.320	1.120
6	1.130	1.086
7	0.124	0.439
8	−1.477	−2.701
9	−0.004	−0.798
10	0.788	1.891
11	0.142	1.717
12	1.403	−2.665
13	0.080	1.628
14	−0.028	−0.045
15	−0.113	−2.473
16	0.595	−0.203
17	0.036	−2.383
18	−1.099	0.085
19	−0.431	2.833
20	−0.434	−2.094
21	0.216	2.163
22	−0.156	0.805
23	−1.266	−1.961
24	−0.956	2.683
25	1.332	1.808

*Data taken from reference 15 and adjusted such that the origin is at the beginning of the amino acid sequence of the α1 chain.

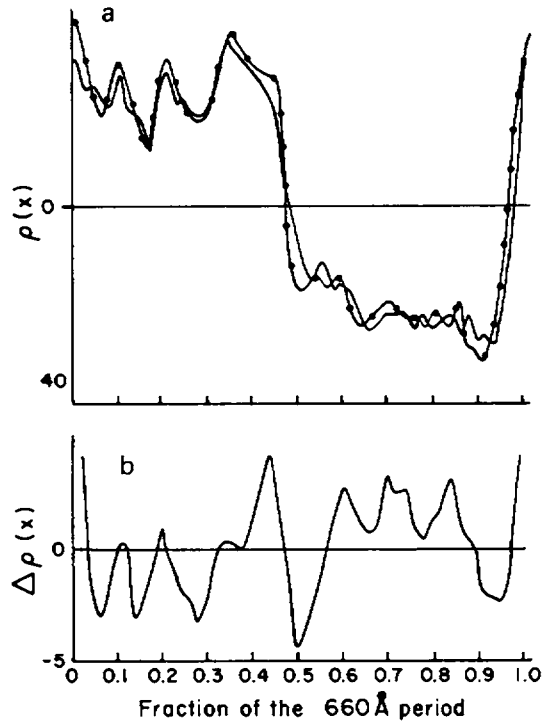

FIGURE 1 (*a*) Fourier transform of ruthenium red-stained (•) and unstained (–) RTT using Claffey's phases (14). (*b*) Electron density difference of the stained and unstained using Claffey's phases.

c_2, a_4, and d bands of PTA- and uranyl acetate-stained native collagen. Since they represent MPS along the collagen fibril, it is reasonable to compare these to the fine striations (shown to be MPS in footnote 2) observed in freeze-etched studies. Three of the four striations observed for RTT at c_2, a_4, e_2, and d match in position. This would mean that the phases obtained from the amino acid sequence of the α1 chain is satisfactory for low resolution work, and that the conformation of the telopeptides and the difference in amino acids of the α2 chain do not make any major contributions.

To determine whether the peaks we obtained from the difference Fourier transform calculations corresponded to stained bands or were noise or artifacts, we stained dispersed native RTT fibrils with ruthenium red under similar conditions, and did electron microscope studies of these (Fig. 3). As in the PTA-stained samples, the 640-Å repeat was obvious and each repeat was divided into one light and one dark region. There were seven major stained bands per period. To decide which was the overlap and which was the gap region, we deposited MgO crystals onto freeze-dried native samples, and shadowed them with platinum. Parts of the fibrils that lay behind the MgO crystals would not be shadowed, but were stained. In this way, we could compare stained and shadowed regions of the same fibril. We found that the overlap

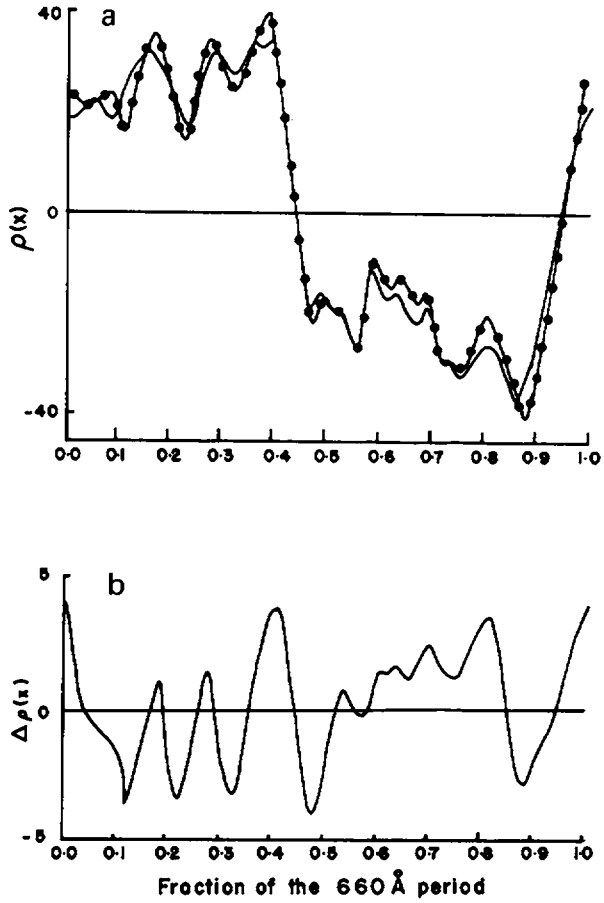

FIGURE 2 (*a*) Fourier transform of ruthenium red-stained (•) and unstained (–) RTT using Hulmes et al.'s phases (15). (*b*) Electron density difference using Hulmes et al.'s phases.

region corresponds to the light zone and the gap to the dark region; Fig. 4 shows an electron micrograph of this. However, we could not tell which end of the overlap region was the N-terminal and which the C-terminal; therefore, we could not decide which end should correspond to the beginning of the period and which to the 0.47 fraction of the period, now known to correspond to the C-terminal end.

If measured in the A → B direction (Fig. 3), the stained bands were situated at 0.00, 0.17, 0.27, 0.40, 0.52, 0.69, and 0.86 fractions of the period. If measured in the B → A direction, they were located at 0,00, 0.11, 0.22, 0.35, 0.52, 0.70, and 0.85 fractions of the period. Comparing with the two plots of the electron density in Fig. 1 and 2, we could obtain better agreement of the peaks with the bands in the A → B direction (Fig. 5). Moreover, the electron density difference obtained by using Hulmes et al.'s phases (15), gave a better matching of the peaks with the stained bands. This indicated that consideration of the telopeptide conformations and inclusion of the amino acids of the $\alpha 2$ chain did affect the Fourier transforms at higher resolution.

It is necessary to point out that there is a difference in contrast between samples only

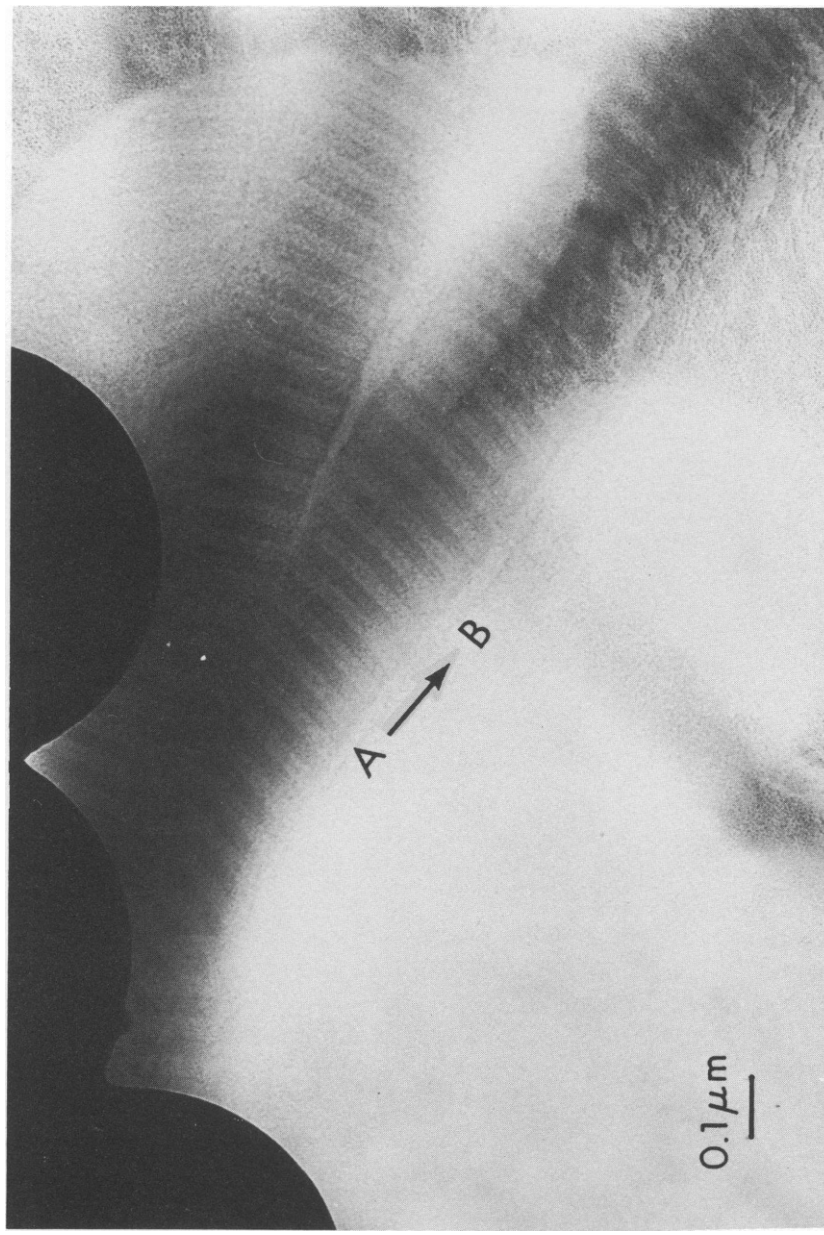

FIGURE 3 Electron micrograph of ruthenium red-stained native RTT fibrils.

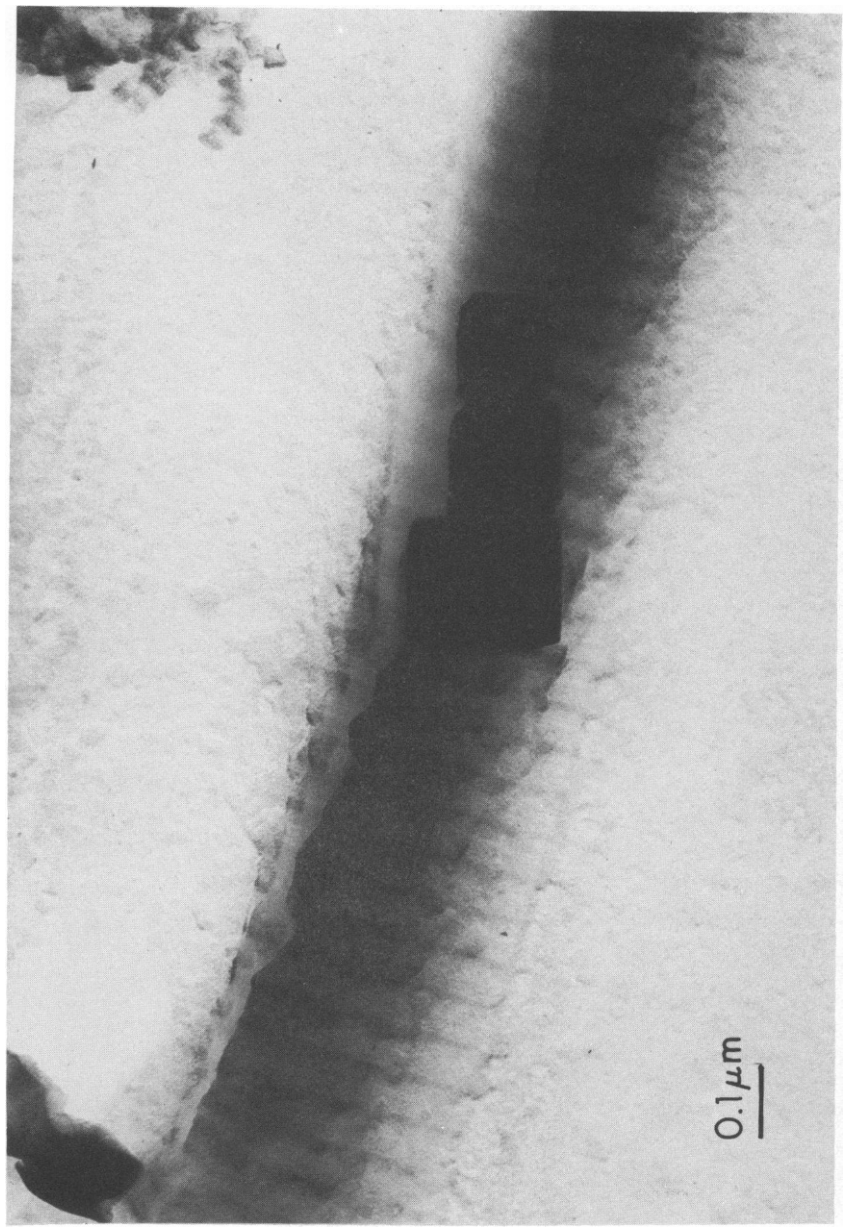

FIGURE 4 Electron micrograph of ruthenium red-stained and partly shadowed RTT fibrils.

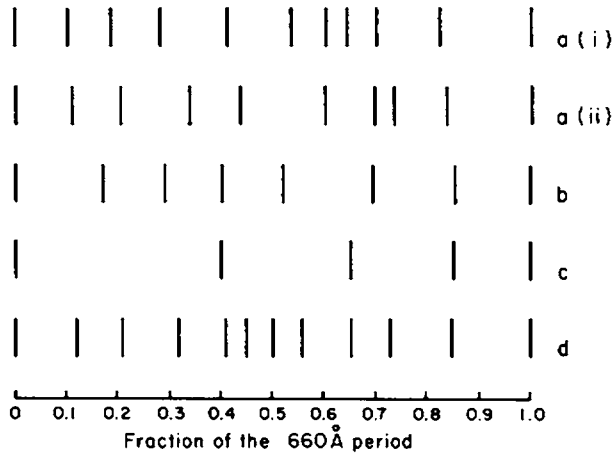

FIGURE 5 A schematic diagram comparing positions of: (*a*) peak positions as obtained by difference Fourier transform calculations using (*i*) Hulmes et al.'s phases and (*ii*) Claffey's phases; (*b*) ruthenium red-stained native RTT, (*c*) fine striations observed in freeze-etched samples, and (*d*) PTA- and uranyl acetate-stained bands.

stained with ruthenium red and those prefixed with osmium and then stained with ruthenium red. Standard procedures, e.g. Luft's ruthenium red-staining method (23), call for fixation of the samples with osmium before ruthenium red staining. Samples thus treated show sharp bands, due to ruthenium red as well as osmium, whereas samples stained without fixation show that the stain does not interact very strongly with the sample. However, prefixing our samples by osmium was not really desirable for two reasons. First, although the mechanism of fixation is not well understood, it obviously involves addition of the heavy metal osmium ions. In fact, fixing with osmium alone results in the development of a band pattern. It has been found that fixing collagen fibrils changes the intensity distribution in SAXD patterns. This means a change in electron density distribution along the collagen axis. Not only would some change result from the added electrons of the osmium, but the fixation may result in possible clumping or spreading of the matrix material and internal redistribution of electron density within the collagen fibrils. Secondly, there is very little observable difference in the published micrographs between osmium-fixed and osmium-fixed and ruthenium red-stained fibrils, suggesting that most of the electron-dense regions are primarily due to the osmium and therefore do not necessarily indicate the location of the MPS. The authors (3), however, claimed that the d – a_4 region was more electron dense. Artifacts would be produced if the ruthenium red is interacting with the deposited osmium and not really with the MPS. Thus, for our purpose, all ruthenium red staining was carried out without prior fixation.

Since ruthenium red is a rather large hexavalent cation (25), there was concern as to whether it would penetrate well into the center of the intact tendon and stain the collagen fibrils uniformly. To check the penetration of this stain, ruthenium red-stained samples for the SAXD experiments were embedded and microtomed. It was found that the stain did penetrate well into the tendon and the tendons were stained uniformly. An electron micrograph of this is shown in Fig. 6.

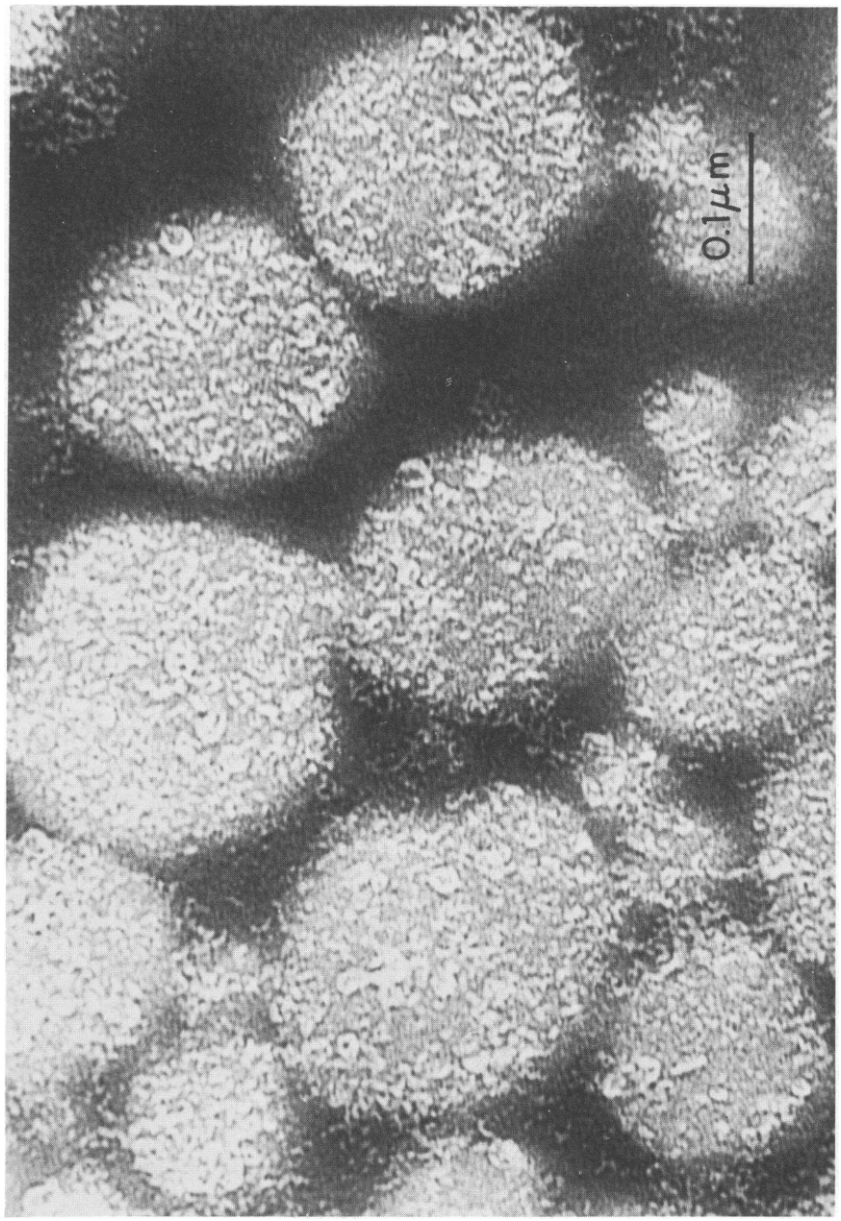

FIGURE 6 Electron micrograph of ruthenium red-stained thin section of RTT.

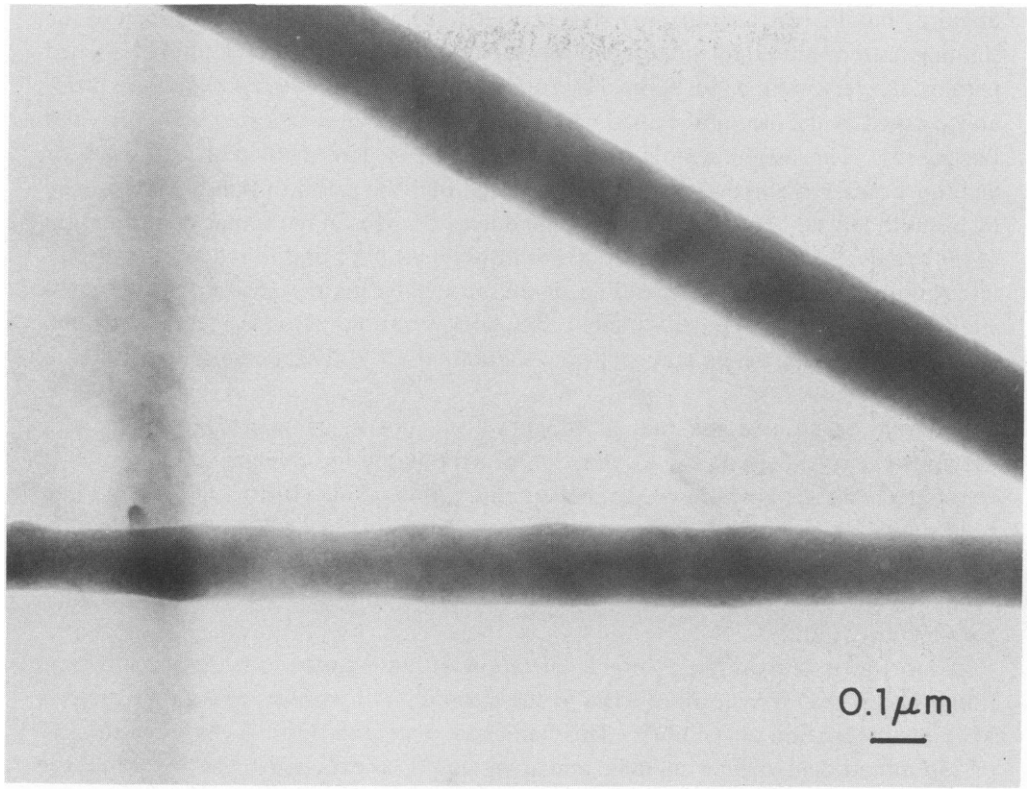

FIGURE 7 Electron micrograph of ruthenium red-stained reconstituted RTT collagen fibrils.

To check the possibility that ruthenium red is not an MPS-specific stain and that it is staining the collagen as well, we stained reconstituted collagen fibrils from RTT and native collagen fibrils with ruthenium red at pH 7. Electron micrographs of the former did not show any staining pattern (Fig. 7), whereas those of the latter gave seven stained bands (Fig. 3).

Some of the stained peaks from the difference Fourier transform calculations should correspond to the fine striations found by freeze-etching which were removable by MPS-specific enzymes, as reported in footnote 2. These are c_2, a_4, e_2, and d bands (Fig. 5). Not all the ruthenium red-stained peaks have to be structures observable with the freeze-etching technique, though. Some of these bands may correspond to MPS located in the interior of the collagen fibril. These may or may not be resolvable by freeze-etching. The disagreement between the stained and freeze-etched data we observed may also be a consequence of the staining method used. Even though the ruthenium red did not give any stain bands with the reconstituted material, there is still the possibility that non-MPS materials in the native fibrils were stained. However, as mentioned before, a new stain or staining method that does not destroy the native structure is needed before improvements can be made in this direction.

The assignment of the peaks partially agrees with the osmium fixed-, ruthenium red-stained MPS data of Nakao and Bashey (3). They reported that the region between the

d and a_4 bands, i.e. the gap, was stained by ruthenium red. However, because the staining pattern caused by the osmium was superimposed on the ruthenium red-stained pattern, the very weak bands stained by ruthenium red in the overlap region are probably masked by the osmium-stained bands, and were thus not reported by Nakao and Bashey (3). The assignment is also not in complete agreement with the work of Serafini-Fracassini and Smith (6), who suggested that the a and b_1 bands were stained by bismuth nitrate. This difference may be due to changes in molecular conformation of the proteoglycans (which contain MPS) at different pH's and in reactions with different stains. Clumping or spreading of the proteoglycans may occur with different staining procedures. Under different salt concentrations, Ruggeri et al. (1) had shown that proteoglycans may appear as granular or rod-shaped particles in thin sections.

It should be pointed out that although we are not in complete agreement with previous workers (3, 6) on the localization of MPS along the collagen axis, there is at least agreement as to the presence of MPS in the region of the a band. The a band had been suggested to be important in the lateral aggregation of collagen fibrils in skin and tendon (26–28). Several investigators had found that in human skin and RTT and similar tissues of other species, the a band was often continuous across several antiparallel fibrils (26, 27).

Of more interest than the general localization within the a band is the specific location in the SAXD transform of MPS at the a_4 band. All workers agree that there is MPS on this portion of the fibril. This band has an overall positive charge in the 234 or 236 amino acid stagger models, and thus would be expected to be favorable for MPS interaction. The presence of MPS along the a_4 band is important because this portion of the period is the site of the C-terminal telopeptides (16). The telopeptides corresponding to the c_2 and a_4 positions have been found to be necessary for normal (660 Å period) collagen fibril formation (29). Removal of these regions results in abnormal fibril formation (29). MPS have also been suggested to stabilize and influence fibril formation (30–34). Since both the C-terminal and the MPS are important in fibril formation and regulation, the location of MPS at this site should be of great biological significance. Since the N-terminal telopeptides have also been suggested to be important for fibril formation, the location of the MPS at this portion (c_2) may also be significant.

The phases calculated by the Hodge-Petruska model may be improved. This would depend on the completion of the sequencing of the $\alpha 2$ chain, and a better understanding of the biochemistry and molecular conformation of the MPS and disaccharides attached to the collagen. Since the amino acid composition of the $\alpha 2$ chain is slightly different (35), the addition of the entire $\alpha 2$ chain to the model should give more accurate phases. In addition, we may improve the model by adding four to seven rows of MPS at specific sites e.g. c_2, a_4 e_2, and d etc., and, as a result, improve the collagen profile.

In both cases it has been assumed that the entire fibril (apart from the terminal regions in the case of Hulmes et al. [15]) is a perfect 10_3 helix. If more is known about the three-dimensional structure of the fibril, then a three-dimensional model can be built instead of the limited axially projected structure.

Two disaccharide units have been reported at number 103 and 943 of the amino acid sequence of the α1 chain of collagen (36). If the chains are staggered by 236 amino acids (or 234), then these units would be at the a_4- and c_2-band positions. These disaccharides are ~7 Å thick and 15 Å wide (36). If they reside outside of each tropocollagen molecule, there could conceivably be a locus of these disaccharides on the periphery of the fibrils. However, even if this were the case, it is doubtful whether they could be observed in the freeze-etched replicas. Thus, the fine striations observed at the a_4 and c_2 positions are not due to the disaccharides.

On the other hand, this locus of disaccharides could be stained by ruthenium red, and contribute to the staining pattern at these two positions. However, because of the presence of MPS observed by freeze etching at the a_4 and c_2 bands, only some of the staining at these two positions may be attributed to the disaccharides, if they do indeed get stained.

At this point, no explanation can be given as to why the MPS are specifically attached to the bands other than the c_2 and a_4 bands.

In conclusion, the freeze-etching and SAXD data indicate that there are at least four and as many as seven bands of MPS along the collagen axis. Comparison of the results with the two techniques indicates that the four most significant of these bands, namely, the ones corresponding to the c_2, a_4, e_2, and d positions, circumscribe the collagen fibrils.

The phases obtained by Claffey (14) using only the α1 chain of collagen are suitable for low resolution work. For higher resolution, the α2 chain, as well as the specific geometry of the telopeptides and the disaccharides as done in part by Hulmes et al. (15), will have to be considered. The apparent qualitative agreement between the MPS axial distribution derived from the SAXD data with the electron microscope image of MPS-stained samples and the freeze-etched evidence provides some evidence supporting the validity of the model phases, and also suggests that our assumption that the MPS contributes only slightly to the projected axial density is appropriate.

Received for publication 2 September 1977 and in revised form 13 July 1978.

REFERENCES

1. RUGGERI, A., C. DELL'ORBO, and A. QUACCI. 1975. Electron microscopic visualization of proteoglycans with Alcian blue. *Biochem. J.* **7**:187.
2. EISENSTEN, R., and K. KNETTNER. 1976. The ground substances of the arterial wall. II. Electron microscope studies. *Atherosclerosis* **27**:37.
3. NAKAO, K., and R. I. BASHEY. 1972. Fine structure of collagen fibrils as revealed by ruthenium red. *Exp. Mol. Pathol.* **17**:6.
4. TORP, S. 1974. Structure-property relationships in tendon. Ph.D. Thesis, Case Western Reserve University, Cleveland, Ohio.
5. MYERS, D. B., T. C. HIGHTON, and D. G. RAYNS. 1969. Acid mucopolysaccharides closley associated with collagen fibrils in normal human synovium. *J. Ultrastruct. Res.* **28**:203.
6. SERAFINI-FRACASSINI, A., and J. W. SMITH. 1966. Observations on the morphology of the protein-polysaccharide complex of bovine nasal cartilage and its relationship to collagen. *Proc. R. Soc. Lond. B Biol. Sci.* **165**:440.
7. KAESBURG, P., and M. M. SHURMAN. 1953. Further evidence concerning the periodic structure in collagen. *Biochim. Biophys. Acta.* **11**:1.
8. TOMLIN, S. G., and C. R. WORTHINGTON. 1956. Low angle X-ray diffraction patterns of collagen, *Proc. R. Soc. Edinb. Sect. A (Math. Phys. Sci.).* **235**:189.

9. ERICSON, L. G., and S. G. TOMLIN. 1959. Further studies of low angle diffraction patterns of collagen. *Proc. R. Soc. Edinb. Sect. A (Math. Phys.Sci.).* **252**:197.
10. ELLIS, D. O., and S. MCGAVIN. 1970. The structure of collagen- an x-ray study. *J. Ultrastruct Res.* **32**:191
11. CHANDROSS, R. J., and R. S. BEAR. 1973. Improved profiles of electron density distribution along collagen fibrils. *Biophys. J.* **13**:1030.
12. HULMES, D. J. S., A. MILLER, D. A. D. PARRY, K. A. PIEZ, and J. WOODHEAD-GALLOWAY. 1974. Analysis of the primary structure of the amino acid sequences of collagen. *J. Mol. Biol.* **79**:137.
13. WALTON, A. G. 1974. Macromolecular aspects of calcified tissues. *J. Biomed. Mater. Res. Biomed. Mater. Symp.* **5**:409.
14. CLAFFEY, W. 1977. Interpretation of the SAXD of collagen in view of the primary structure of the α1 chain. *Biophys. J.* **19**:63.
15. HULMES, D. J. S., A. MILLER, S. W. WHITE, and B. B. DOYLE. 1977. Interpretation of the meridional x-ray diffraction pattern from collagen fibres in terms of the known amino acid sequence. *J. Mol. Biol.* **110**:643
16. BRUNS, R. R., and J. GROSS. 1973. Band pattern of the segment-long-spacing form of collagen. Its use in the analysis of primary structure. *Biochemistry.* **12**:808.
17. BRUNS, R. R., R. L. TRESTAD, and J. GROSS. 1973. Cartilage collagen: A staggered substructure in reconstituted fibrils. *Science (Wash. D.C.).* **181**:269.
18. CHAPMAN, J. A. 1974. Amino acid sequence of collagen and stained bands. Conn. Tis. Res. **2**:137.
19. CHAPMAN, J. A. and R. A. HARDCASTLE. 1974. Computer matching of stained bands of collagen and amino acids and stain simulation. *Connect. Tissue Res.* **2**:151.
20. SPIRO, R. G. 1969. Characterization and quantitative determination of the hydroxylysine-linked carbohydrate units of several collagens. *J. Biol. Chem.* **244**:602.
21. BUTLER, W. T. 1970. Chemical studies on cyanogen bromide peptides of rat skin collagen. Covalent structure of α1-CB5, the major hexose-containing cyanogen bromide peptide of α1. *Biochemistry* **9**:44.
22. BOUTEILLE, M., and D. C. PEASE. 1971. The 3-dimensional structure of native collagenous fibrils. *J. Ultrastruct Res.* **35**:314.
23. LUFT, J. H. 1971. Ruthenium red and violet. I. (Chemical purification methods of use for electron microscopy and mechanism of action). *Anat. Rec.* **171**:347.
24. LUFT, J. H. 1964. Electron microscopy of cell extraneous coats as revealed by ruthenium red. *J. Cell Biol.* **23**:54A. (Abstr.)
25. HAYAT, M. A. 1975. *In* Positive Staining for Electron Microscopy. Van Nostrand Reinhold Company, New York. 162.
26. GIESEKING, R. 1962. Electron microscope observations on the arrangement of elementary collagen fibrils in the tendon fiber. *Z. Zellforsch. Mikrosk. Anat.* **58**:160.
27. BRAUN-FALCO, O., and M. RUPEC. 1964. Some observations on dermal collagen fibrils in ultra-thin sections. *J. Invest. Dermatol.* **42**:15.
28. BORYSKO, E. 1963. *In* Ultrastructure of Protein Fibers. R. Boraksy, editor. Academic Press, Inc., New York. 19.
29. LEIBOVICH, S. J., and J. B. WEISS. 1970. Electron microscope studies of the effects of endo- and exopeptidase digestion on tropocollagen. A novel concept of the role of terminal regions in fibrilogenesis. *Biochim. Biophys. Acta.* **214**:445.
30. TOOLE, B. P., and D. A. LOWTHER. 1968. Effect of chondroitin sulfate-protein on the formation of collagen fibrils *in vitro*. *Biochem. J.* **109**:857.
31. MATHEWS, M. B. 1965. Interaction of collagen and acid mucopolysaccharides—connective tissues. *Biochem. J.* **76**:710.
32. MATHEWS, M. B., and L. DECKER. 1968. The effect of acid mucopolysaccharides and acid mucopolysaccharide-proteins on fibril formation from collagen solutions. *Biochem. J.* **109**:517.
33. KEECH, M. K. 1961. Formation of fibrils from collagen solution. IV. Effect of mucopolysaccharides and nucleic acids. *J. Biophys. Biochem. Cytol.* **9**:193.
34. WOOD, G. C. 1960. Formation of fibrils from collagen solutions. III. Effect of chondroitin sulfates and other naturally occuring polyanions on the rate of formation. *Biochem. J.* **75**:605.
35. PIEZ, K. A., G. BALIAN, E. M. CLICK, and P. BORNSTEIN. 1972. Homology between α1 and α2 chains of collagen. *Biochem. Biophys. Res. Commun.* **48**:990.
36. MORGAN, P. H., G. JACOBS, and S. CUNNINGHAM. 1970. A comparative study of glycoproteins derived from selected vertebrate collagens. *J. Biol. Chem.* **245**:5042.